

On the Recurrence Coefficients for the q -Laguerre Weight and Discrete Painlevé Equations

Jie Hu

Department of Mathematics, Jinzhong University, Yuci District, Jinzhong, Shanxi, China

E-mail: hujie_0610@163.com

Anton Dzhamay*

Beijing Institute of Mathematical Sciences and Applications (BIMSA), Beijing, China and

School of Mathematical Sciences, The University of Northern Colorado, Greeley, CO 80526, USA

E-mail: adzham@bimsa.cn

Yang Chen

Faculty of Science and Technology, Department of Mathematics, University of Macau, Avenida da Universidade, Taipa, Macau, China

E-mail: chenyayang57@gmail.com

Abstract

We study the dependence of recurrence coefficients in the three-term recurrence relation for orthogonal polynomials with a certain deformation of the q -Laguerre weight on the degree parameter n . We show that this dependence is described by a discrete Painlevé equation on the family of $A_5^{(1)}$ Sakai surfaces, but this equation is different from the standard examples of discrete Painlevé equations of this type and instead is a composition of two such. This case study is a good illustration of the effectiveness of a recently proposed geometric identification scheme for discrete Painlevé equations.

Keywords: orthogonal polynomials, Painlevé equations, difference equations, birational transformations.

MSC2020: *Primary:* 33C45, 34M55, 14E07; *Secondary:* 39A45, 33D45, 39A13

1 Introduction

Orthogonal polynomials play an important role in many fields of Mathematics and Mathematical Physics, such as the Random Matrix Theory [Meh04], Approximation Theory, Stochastic Processes, and others. They form a natural basis for expansions of solutions of partial differential or difference equations. There are many connections between orthogonal polynomials and Painlevé equations, see the recent monograph [VA18] and the references therein. In particular, for semi-classical weights, coefficients of the three-term recurrence relation for discrete and continuous orthogonal polynomials with respect to the semi-classical weight satisfy Painlevé-type equations, that can be both differential equations w.r.t. one of the parameters in the weight function, [Mag95], or discrete w.r.t. the degree n of the polynomial, see many examples in [VA22].

One common issue in working with discrete or differential Painlevé equations is that of the coordinates — the same dynamic can take a very simple or a very complicated form based on the choice of a coordinate system. This also makes matching the equation with some of the standard examples a very nontrivial task. Arguably the most effective approach to this problem is provided by the algebro-geometric approach to Painlevé equations that is primarily due to H. Sakai, [Sak01]. In this approach the coordinates can be essentially removed from the picture and the equation corresponds to a conjugacy class of a translation element in some affine Weyl group (the symmetry group of the equation). From that point of view, different choices of coordinates correspond to different geometric realizations of the configuration spaces for the same dynamic. The identification question can then be answered on the purely algebraic level, which can be further extended to the construction of an explicit change of coordinates reducing the equation in question to some standard form.

*Corresponding author

This procedure was formalized in [DFS20], and since then a few more examples were considered using this approach, e.g., [LDFZ22], [DFS22], as well as our previous paper [HDC20] where we considered the Laguerre unitary ensemble defined by the weight $w(x; \alpha) = x^\alpha e^{-x}$, over $[0, t]$ and showed that its recurrence coefficients satisfy one of the standard difference Painlevé equations on the $D_5^{(1)}$ -family of Sakai surfaces. In the present paper we consider the q -difference case defined by the deformed q -Laguerre weight (1.1), supported on $[0, \infty)$, introduced by Chen and Griffin [CG15],

$$w(x, \alpha, t; q) = \frac{x^\alpha}{((q-1)x; q)_\infty ((q-1)\frac{t}{x}; q)_\infty}, \quad t \geq 0, \alpha > -1, 0 < q < 1, \quad (1.1)$$

where $(a; q)_\infty$ is the usual q -Pochhammer symbol

$$(a; q)_\infty := \prod_{j=0}^{\infty} (1 - aq^j).$$

The physical motivation to consider such a weight is the following. First, in the limit as $t \rightarrow 0^+$ this weight reduces to the q -Laguerre weight [Moa81], and so the weight (1.1) is a one-parameter deformation of this q -Laguerre weight. If we set $\alpha = 0$ and $t = q/(1-q)^2$, the corresponding orthogonal polynomials are the Stieltjes-Wigert polynomials and the weight essentially becomes log-normal, i.e., $w(x) = \exp(-c(\ln(x))^2)$, where $c > 0$, which is related to a physical problem of localization. Moreover, this weight generates the indeterminate moment problems, namely, the same set of moments are generated by different weights. For $\alpha \neq 0$, the corresponding orthogonal polynomials were considered by Askey [Ask89]. For more details, please see [CG15], as well as [CL98, Section 2], and references therein.

Special cases of this weight are also known to be related with Painlevé and discrete Painlevé equations. In particular, in the limit as $q \rightarrow 1^-$ this weight transforms to the weight $x^\alpha e^{-x} e^{-t/x}$, in which case the recurrence coefficients are related to solutions of the Painlevé III equation w.r.t. the t -variable, [CI10], and also satisfy one of the standard discrete Painlevé equations on the $D_6^{(1)}$ surface w.r.t. discrete degree variable n , [LDFZ22]. And for the semiclassical variation of the q -Laguerre weight

$$\frac{x^\alpha (-p/x^2; q^2)_\infty}{(-x^2; q^2)_\infty (-q^2/x^2; q^2)_\infty}, \quad x \in [0, \infty), p \in [0, q^{-\alpha}], a \geq 0, \quad (1.2)$$

and the q -analogue of the Laguerre weight $\frac{x^\alpha}{(-x^2; q^2)_\infty}$, the recurrence coefficients can be expressed in terms of solution of the q -Painlevé V equation [BVA10, BVA15]. Thus, understanding the type of discrete Painlevé equations governing the dynamic of recurrence coefficients for this generalized weight is a very interesting question. In [CG15], the authors suggested that this can be related to αq -P_{IV} or αq -P_V equations, but this turns out not to be the case. In fact, as we show below, the resulting recurrence corresponds to a new discrete Painlevé equation that is a combination of two standard dynamics. It is very difficult to see such identifications without using the geometric approach proposed in [DFS20].

Let us now briefly review the derivation of the recurrence relation that we are interested in, following [CG15]. Consider a family $\{P_n(x)\}$ of *monic* polynomials of degree n that are orthogonal with respect to the deformed q -Laguerre weight function $w(x, \alpha, t; q)$ (1.1) on $[0, \infty)$:

$$\int_0^\infty P_m(x) P_n(x) w(x, \alpha, t; q) dx = \delta_{m,n} h_n,$$

where $\delta_{i,j}$ is the Kronecker delta and h_n is the square of the L^2 norm of $P_n(x)$ w.r.t. this weight. It is well-known that orthogonal polynomials satisfy the three-term recurrence relation

$$xP_n(x) = P_{n+1}(x) + \alpha_n P_n(x) + \beta_n P_{n-1}(x),$$

with initial conditions $P_{-1}(x) = 0$ and $P_0(x) = 1$. It is convenient to parameterize the recurrence coefficients α_n and β_n that we are interested in using auxiliary variables R_n and r_n by

$$q^{2n+\alpha} \alpha_n = \frac{1 - q^n}{1 - q} + \frac{1 - q^{n+\alpha+1}}{q(1 - q)} + q^{n-1} t (R_n + (1 - q) \sum_{j=0}^{n-1} R_j),$$

$$q^{2n-1}\beta_n = \frac{1}{q^{2\alpha+2n}} \frac{1-q^n}{1-q} \frac{1-q^{n+\alpha}}{1-q} + \frac{1-q^n}{q^{\alpha+1}} t + \frac{q^n}{q^{\alpha+1}} tr_n + \frac{1}{q^{2\alpha+n+1}} t \sum_{j=0}^{n-1} R_j,$$

where

$$R_n = \frac{1}{h_n} \int_0^\infty P_n(y) P_n(y/q) \frac{w(y, \alpha, t; q)}{y} dy,$$

$$r_n = \frac{1}{h_{n-1}} \int_0^\infty P_n(y) P_{n-1}(y/q) \frac{w(y, \alpha, t; q)}{y} dy.$$

The relation with discrete Painlevé equations is then given by the following theorems. First, there are the recurrence relations obtained by Chen and Griffin that describe the evolution, after yet another reparameterization, of the variables R_n and r_n .

Theorem 1 ([CG15, Theorem 1.4]). *Let*

$$x_n = \frac{q^{n+\alpha}(1-q)}{R_n}, \quad y_n = q^n(1-r_n), \quad T = \frac{(1-q)^2}{q} t, \quad Q = q^\alpha.$$

Then the quantities x_n and y_n satisfy the following system of difference equations:

$$\begin{cases} (x_n y_n - 1)(x_{n-1} y_n - y_n) = q^{2n} Q T \frac{(y_n - 1)(y_n - 1/T)}{q^n - y_n}, \\ (x_n y_n - 1)(x_n y_{n+1} - 1) = -q^{2n+1} Q \frac{(x_n - 1)(x_n - T)}{x_n}. \end{cases} \quad (1.3)$$

Our main result is the identification of this dynamic with a discrete Painlevé equation on the $A_5^{(1)}$ -family of Sakai surfaces (that is different from possible discrete Painlevé equations suggested in [CG15]). Recall that the full symmetry group of the $A_5^{(1)}$ -family of Sakai surfaces is the extended affine Weyl group of type $E_3^{(1)}$ (that is sometimes also denoted by $(A_2 + A_1)^{(1)}$). This group is described by a *disconnected* Dynkin diagram shown on Figure 1 (on the right).

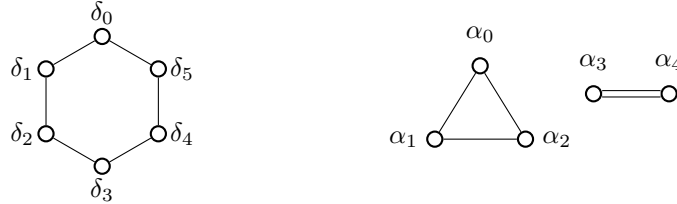


Figure 1: Affine Dynkin diagrams of type $A_5^{(1)}$ (left) and $E_3^{(1)}$ (right).

There are two standard examples of discrete Painlevé equations on this surface family that naturally correspond to translation elements on one of the connected components of the Dynkin diagram $E_3^{(1)}$. The first translation acts on the symmetry root lattice as

$$\psi_* : \alpha = \langle \alpha_0, \alpha_1, \alpha_2; \alpha_3, \alpha_4 \rangle \mapsto \psi_*(\alpha) = \alpha + \langle 0, 0, 0; -1, 1 \rangle \delta, \quad (1.4)$$

and so is a translation on the $A_1^{(1)}$ -sublattice, and the second one as

$$\phi_* : \alpha = \langle \alpha_0, \alpha_1, \alpha_2; \alpha_3, \alpha_4 \rangle \mapsto \phi_*(\alpha) = \alpha + \langle 0, 1, -1; 0, 0 \rangle \delta, \quad (1.5)$$

and so is a translation on the $A_2^{(1)}$ -sublattice. Based on the translation vectors (actually, their equivalence classes), we use the notation $[000\bar{1}1]$ and $[01\bar{1}00]$ for these two translation dynamics. The dynamic $[000\bar{1}1]$

is also known as a q - P_{IV} equation since it has a continuous limit to the standard differential P_{IV} equation, and for the similar reason the dynamic $[01\bar{1}00]$ is known as the q - P_{III} equation, see [Sak01]. The existence of such continuous limits can be also seen from the degeneration cascade in the Sakai classification scheme shown on Figure 2.

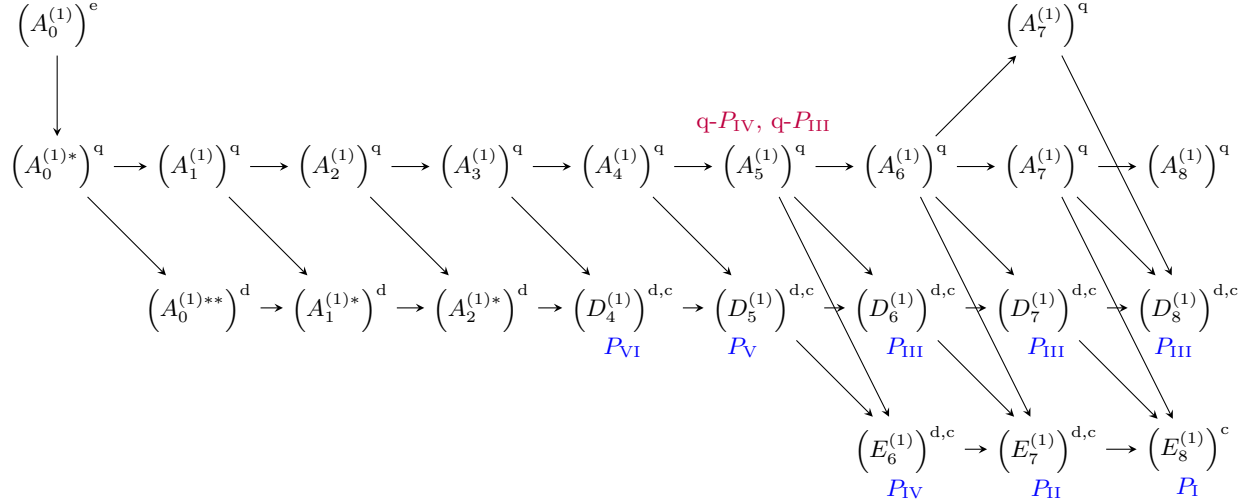


Figure 2: Surface-type classification scheme for Painlevé equations

In [KNY17] the authors gave a careful description of the standard realizations of Sakai surfaces for each of the cases shown on Figure 2, and it became the standard reference on this subject. For the $A_5^{(1)}$ -family of surfaces there are two such realizations: the (a)-model [KNY17, 8.2.7] is better suited for the dynamic (1.4) and the (b)-model [KNY17, 8.2.10] for the dynamic (1.5). Of course, both families are birationally equivalent. To make the paper self-contained, we briefly describe them in Section 2.

In contrast to many other examples of discrete Painlevé equations that occur in the study of orthogonal polynomials, the recurrence (1.3) is not conjugated to any of these two standard equations and instead is essentially their composition with translations in both components. Namely, our main result is the following Theorem.

Theorem 2. *The discrete dynamic given by (1.3) defines a discrete Painlevé equation $[01\bar{1}\bar{1}1]$ on the $A_5^{(1)}$ family of Sakai surfaces that is equivalent to the composition $\psi \circ \phi = \phi \circ \psi$ of two standard mappings.*

We prove this Theorem, as well as give the explicit form of the mapping (3.14) on the standard (b)-model realization of the $A_5^{(1)}$ -family and the explicit birational change of coordinates (3.13) transforming our dynamic to this form, in Section 3.

It is easy to see that the mappings ϕ , ψ , and φ are non-conjugate. Indeed, for that it is enough to look at the Jordan block structure of the induced linear maps on the Picard lattice. For equation $[000\bar{1}1]$ it is $J(-1, 1)^{\oplus 3} \oplus J(1, 1)^{\oplus 4} \oplus J(1, 3)$, for equation $[01\bar{1}00]$ it is $J(1, 1)^{\oplus 3} \oplus J(1, 3) \oplus J(e^{2\pi i/3}, 1)^{\oplus 2} \oplus J(e^{4\pi i/3}, 1)^{\oplus 2}$, and for equation $[01\bar{1}\bar{1}1]$ it is $J(-1, 1) \oplus J(1, 1)^{\oplus 2} \oplus J(1, 3) \oplus J(e^{\pi i/3}, 1) \oplus J(e^{2\pi i/3}, 1) \oplus J(e^{4\pi i/3}, 1) \oplus J(e^{5\pi i/3}, 1)$.

Remark 3. *Given that the equation $[000\bar{1}1]$ has a continuous limit to the standard differential P_{IV} equation and the equation $[01\bar{1}00]$ has a continuous limit to the standard differential P_{III} equation, it would be very interesting to see if the equation $[01\bar{1}\bar{1}1]$ has a good continuous limit. We plan to consider this question in the follow-up work.*

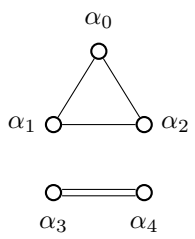
The paper is organized as follows. In Section 2 we collect some basic data about the q -P $(E_3^{(1)}/A_5^{(1)})$ surface families, and in Section 3 we perform the detailed study of recurrence (1.3), along the lines of [DFS20], and establish our main result. The final section is a brief conclusion.

2 Discrete Painlevé Equations on the q -P $\left(E_3^{(1)}/A_5^{(1)}\right)$ Surfaces

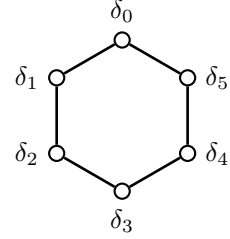
To make the paper self-contained, we begin by briefly describing some basic geometric data for discrete Painlevé equations for the $A_5^{(1)}$ surface family, following [KNY17]. We also give birational representations of the extended affine Weyl symmetry group $\tilde{W}\left(E_3^{(1)}\right)$, which is essentially the same as in [KNY17], but some maps differ by a choice of normalizations. There are two natural realizations of the $A_5^{(1)}$ -family via the configuration of the blow-up points: the (a)-model [KNY17, 8.2.7] and the (b)-model [KNY17, 8.2.10]. We begin with the (a)-model.

2.1 The q -P $\left(E_3^{(1)}/A_5^{(1)}; a\right)$ Surface Family

This family corresponds to the choice of root bases for the surface and symmetry sub-lattices shown on Figure 3.



$\alpha_0 = \mathcal{H}_f + \mathcal{H}_g - \mathcal{E}_{2367},$
 $\alpha_1 = \mathcal{H}_f + \mathcal{H}_g - \mathcal{E}_{1468},$
 $\alpha_2 = \mathcal{E}_6 - \mathcal{E}_5,$
 $\alpha_3 = \mathcal{H}_f + 2\mathcal{H}_g - \mathcal{E}_{123568}$
 $\alpha_4 = \mathcal{H}_f - \mathcal{E}_{47},$



$\delta_0 = \mathcal{H}_f - \mathcal{E}_{12},$
 $\delta_1 = \mathcal{E}_2 - \mathcal{E}_3,$
 $\delta_2 = \mathcal{H}_g - \mathcal{E}_{24},$
 $\delta_3 = \mathcal{H}_f - \mathcal{E}_{56},$
 $\delta_4 = \mathcal{H}_g - \mathcal{E}_{17},$
 $\delta_5 = \mathcal{E}_1 - \mathcal{E}_8;$

(2.1)

Figure 3: The symmetry (left) and the surface (right) root bases for the q -P $\left(E_3^{(1)}/A_5^{(1)}; a\right)$

2.1.1 The point configuration

The decomposition of the anti-canonical divisor class into the classes of irreducible components δ_i above,

$$-\mathcal{K}_{\mathcal{X}} = [H_f - E_1 - E_2] + [E_2 - E_3] + [H_g - E_2 - E_4] + [H_f - E_5 - E_6] + [H_g - E_1 - E_7] + [E_1 - E_8],$$

can be realized by the point configuration on Figure 4. In [KNY17] all q -type configurations are parameterized using the same set of 10 parameters $\kappa_1, \kappa_2, \nu_1, \dots, \nu_8$. Using these parameters, in case (a) the points are

$$p_1 \left(\frac{1}{f} = 0, g = 0 \right) \leftarrow p_8 \left(\frac{1}{f} = 0, fg = -\frac{\kappa_1}{\nu_1 \nu_8} \right), p_2 \left(\frac{1}{f} = 0, \frac{1}{g} = 0 \right) \leftarrow p_3 \left(\frac{1}{f} = 0, \frac{f}{g} = -\nu_2 \nu_3 \right),$$

$$p_4 \left(f = \nu_4, \frac{1}{g} = 0 \right), p_5 \left(f = 0, g = \frac{\nu_5}{\kappa_2} \right), p_6 \left(f = 0, g = \frac{\nu_6}{\kappa_2} \right), p_7 \left(f = \frac{\kappa_1}{\nu_7}, g = 0 \right).$$

However, it is easy to see that in this case the true number of parameters is only *four*: using the action of the gauge group of Möbius transformations we can make some of the point coordinates vanish, and there is still a residual two-parameter rescaling acting on the remaining six non-zero coordinates. As usual, it is convenient to consider the canonical parameters known as the *root variables*.

Recall that *root variables* a_i are computed using the *period map* $\chi : \text{Span}_{\mathbb{Z}}\{\alpha_i\} \rightarrow \mathbb{C}$, see [Sak01] or [DT18] for details. In this case the period map is defined using the symplectic form $\omega = \frac{df \wedge dg}{fg}$ and the root variables $a_i = \exp(\chi(\alpha_i))$ for this configuration can be expressed in terms of the above parameters as

$$a_0 = \frac{\kappa_1 \kappa_2}{\nu_2 \nu_3 \nu_6 \nu_7}, a_1 = \frac{\kappa_1 \kappa_2}{\nu_1 \nu_4 \nu_6 \nu_8}, a_2 = \frac{\nu_6}{\nu_5}, a_3 = \frac{\kappa_1 \kappa_2^2}{\nu_1 \nu_2 \nu_3 \nu_5 \nu_6 \nu_8}, a_4 = \frac{\kappa_1}{\nu_4 \nu_7}. \quad (2.2)$$

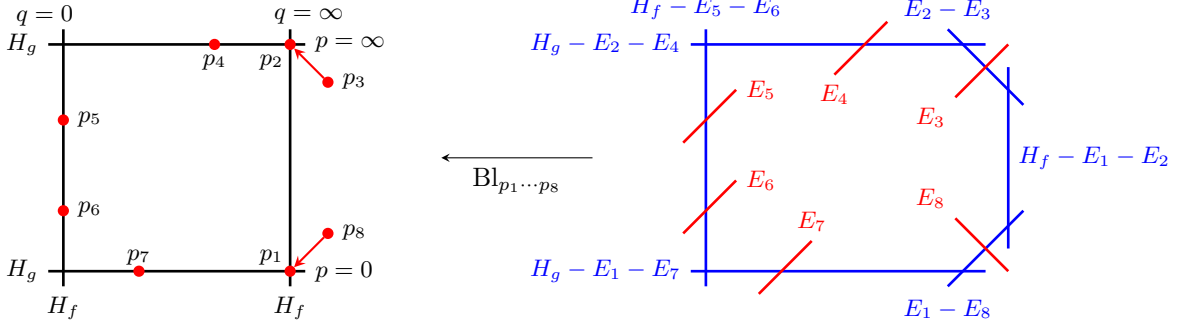


Figure 4: The model type (a) Sakai surface for the $q\text{-P}\left(E_3^{(1)}/A_5^{(1)}\right)$ family

These root variables satisfy the constraint

$$a_0 a_1 a_2 = a_3 a_4 = \exp(\chi(\delta = -\mathcal{K}\chi)) = q = \frac{\kappa_1^2 \kappa_2^2}{\nu_1 \nu_2 \nu_3 \nu_4 \nu_5 \nu_6 \nu_7 \nu_8}, \quad (2.3)$$

where q is the parameter of the dynamic. We can then express the coordinates of the base points using the root variables,

$$p_1 \left(\frac{1}{f} = 0, g = 0 \right) \leftarrow p_8 \left(\frac{1}{f} = 0, fg = -\frac{a_1 a_4}{a_0} \frac{\nu_4^2}{\nu_2 \nu_3} \right), \quad p_2 \left(\frac{1}{f} = 0, \frac{1}{g} = 0 \right) \leftarrow p_3 \left(\frac{1}{f} = 0, \frac{f}{g} = -\nu_2 \nu_3 \right),$$

$$p_4 \left(f = \nu_4, \frac{1}{g} = 0 \right), \quad p_5 \left(f = 0, g = \frac{a_4}{a_0 a_2} \frac{\nu_4}{\nu_2 \nu_3} \right), \quad p_6 \left(f = 0, g = \frac{a_4}{a_0} \frac{\nu_4}{\nu_2 \nu_3} \right), \quad p_7 (f = a_4 \nu_4, g = 0),$$

where the free parameters $\nu_2 \nu_3$ and ν_4 can be set to 1 using the rescaling action on the coordinate axes.

2.1.2 The extended affine Weyl symmetry group

Recall that, given a Dynkin diagram, the corresponding Weyl group is defined in terms of generators w_i corresponding to the nodes α_i of the diagram, and with edges of the diagram encoding the relations between these generators. For the affine $E_3^{(1)}$, we have

$$W\left(E_3^{(1)}\right) = W\left(\begin{array}{c} \alpha_0 \\ \circ \\ \alpha_1 \circ \alpha_2 \\ \alpha_3 \text{---} \alpha_4 \end{array} \right) = \left\langle w_0, \dots, w_4 \left| \begin{array}{l} w_i^2 = e, \quad w_i \circ w_j = w_j \circ w_i \quad \text{when } \begin{array}{c} \circ \\ \alpha_i \quad \alpha_j \end{array} \\ w_i \circ w_j \circ w_i = w_j \circ w_i \circ w_j \quad \text{when } \begin{array}{c} \circ \text{---} \circ \\ \alpha_i \quad \alpha_j \end{array} \end{array} \right. \right\rangle.$$

In our setting this group is represented via actions on $\text{Pic}(\mathcal{X})$ given by reflections in the roots α_i ,

$$w_i(\mathcal{C}) = w_{\alpha_i}(\mathcal{C}) = \mathcal{C} - 2 \frac{\mathcal{C} \bullet \alpha_i}{\alpha_i \bullet \alpha_i} \alpha_i = \mathcal{C} + (\mathcal{C} \bullet \alpha_i) \alpha_i, \quad \mathcal{C} \in \text{Pic}(\mathcal{X}). \quad (2.4)$$

Next, we need to extend this group by the group of the automorphisms of the Dynkin diagram (that corresponds to some re-labeling of the symmetry/surface roots) $\text{Aut}(E_3^{(1)}) \simeq \text{Aut}(A_5^{(1)}) \simeq \mathbb{D}_6$, where \mathbb{D}_6 is the usual dihedral group of the symmetries of a regular hexagon (note that this group acts on both the symmetry and the surface roots and we describe its action using the standard permutation cycle notation). This group

is generated by the two reflections $\sigma_0 = (\alpha_0\alpha_2)(\alpha_3\alpha_4) = (\delta_0\delta_1)(\delta_2\delta_5)(\delta_3\delta_4)$ and $\sigma_1 = (\alpha_1\alpha_2) = (\delta_0\delta_2)(\delta_3\delta_5)$, and it is convenient to also consider the rotation $\sigma_2 = \sigma_1 \circ \sigma_0 = (\alpha_0\alpha_1\alpha_2)(\alpha_3\alpha_4) = \delta_0\delta_1\delta_2\delta_3\delta_4\delta_5$, see Figure 5.

The action of generators of $\text{Aut}(E_3^{(1)})$ on $\text{Pic}(\mathcal{X})$ can be realized as compositions of reflections in some other roots in the lattice, e.g.,

$$\begin{aligned}\sigma_0 &= w_{\mathcal{E}_5-\mathcal{E}_7} \circ w_{\mathcal{E}_4-\mathcal{E}_8} \circ w_{\mathcal{H}_g-\mathcal{E}_1-\mathcal{E}_2} \circ w_{\mathcal{H}_g-\mathcal{E}_3-\mathcal{E}_6} \circ w_{\mathcal{H}_f-\mathcal{E}_2-\mathcal{E}_6}, \\ \sigma_1 &= w_{\mathcal{E}_5-\mathcal{E}_8} \circ w_{\mathcal{H}_g-\mathcal{E}_4-\mathcal{E}_6} \circ w_{\mathcal{H}_f-\mathcal{E}_1-\mathcal{E}_6}.\end{aligned}$$

The resulting group $\widetilde{W}(E_3^{(1)}) = \text{Aut}(E_3^{(1)}) \ltimes W(E_3^{(1)})$ is called an extended affine Weyl symmetry group and its action on $\text{Pic}(\mathcal{X})$ can be further extended to an action on point configurations by elementary birational maps (which lifts to isomorphisms $w_i : \mathcal{X}_{\mathbf{b}} \rightarrow \mathcal{X}_{\mathbf{b}}$ on the family of Sakai's surfaces); this is known as a *birational representation*. We describe it in the following Lemma.

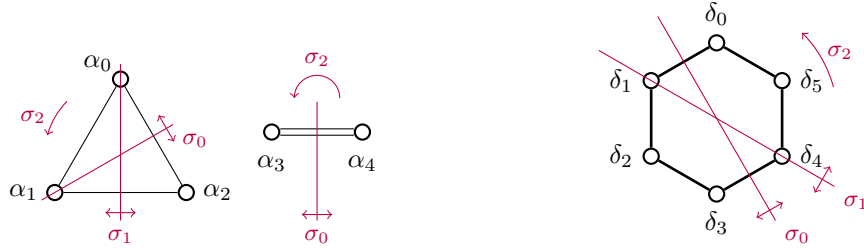


Figure 5: The automorphisms of Dynkin diagrams $E_3^{(1)}$ and $A_5^{(1)}$

Lemma 4. *Generators of the extended affine Weyl group $\widetilde{W}(E_3^{(1)})$ transform an initial point configuration in the (a)-model, expressed in both the KNY parameters and the root variables as*

$$\begin{pmatrix} \kappa_1 & \nu_1 & \nu_3 & \nu_5 & \nu_7 \\ \kappa_2 & \nu_2 & \nu_4 & \nu_6 & \nu_8 \end{pmatrix}; f \sim \begin{pmatrix} a_0 & a_1 & a_2 \\ a_3 & a_4 & \end{pmatrix}; f, \quad (2.5)$$

by changing the parameters and the affine coordinates (f, g) as follows:

$$\begin{aligned}w_0 &: \begin{pmatrix} \kappa_1 & \nu_1 \left(\frac{\nu_2\nu_3\nu_6\nu_7}{\kappa_1\kappa_2} \right)^3 & \nu_3 & \nu_5 & \nu_7 \\ \frac{\nu_2\nu_3\nu_6\nu_7}{\kappa_1} & \nu_2 & \nu_4 & \frac{\kappa_1\kappa_2}{\nu_2\nu_3\nu_7} & \nu_8 \end{pmatrix}; \begin{pmatrix} \frac{\kappa_1\kappa_2 f(\nu_7(f+\nu_2\nu_3g)-\kappa_1)}{\nu_2\nu_3\nu_7(\nu_6(\nu_7f-\kappa_1)+\kappa_1\kappa_2g)} \\ \frac{\kappa_1^2\kappa_2g(\kappa_2(f+\nu_2\nu_3g)-\nu_2\nu_3\nu_6)}{(\nu_2\nu_3)^2\nu_6\nu_7(\nu_6(\nu_7f-\kappa_1)+\kappa_1\kappa_2g)} \end{pmatrix} \\ &\sim \begin{pmatrix} \frac{1}{a_0} & a_0a_1 & a_0a_2 \\ a_3 & a_4 & \end{pmatrix}; \begin{pmatrix} \frac{a_0f(f+g-a_4)}{f+a_0g-a_4} \\ \frac{a_0g(a_0(f+g)-a_4)}{(f+a_0g-a_4)} \end{pmatrix}, \\ w_1 &: \begin{pmatrix} \kappa_1 & \nu_1 \left(\frac{\kappa_1\kappa_2}{\nu_1\nu_4\nu_6\nu_8} \right)^3 & \nu_3 & \nu_5 & \nu_7 \\ \kappa_2 \left(\frac{\kappa_1\kappa_2}{\nu_1\nu_4\nu_6\nu_8} \right)^2 & \nu_2 & \nu_4 & \frac{\kappa_1\kappa_2}{\nu_1\nu_4\nu_6} & \nu_8 \end{pmatrix}; \begin{pmatrix} \frac{\nu_4\nu_6f(\nu_1\nu_8(f-\nu_4)g+\kappa_1)}{\kappa_1(\kappa_2(f-\nu_4)g+\nu_4\nu_6)} \\ \frac{(\nu_1\nu_6\nu_8)^2\nu_4g(\kappa_2(f-\nu_4)g+\nu_4\nu_6)}{\kappa_1\kappa_2^2((\nu_1\nu_6\nu_8f-\kappa_1\kappa_2)g+\kappa_1\nu_6)} \end{pmatrix} \\ &\sim \begin{pmatrix} a_0a_1 & \frac{1}{a_1} & a_1a_2 \\ a_3 & a_4 & \end{pmatrix}; \begin{pmatrix} \frac{f(a_0(f-1)g+a_1a_4)}{a_1(a_0(f-1)g+a_4)} \\ \frac{g(a_0(f-1)g+a_4)}{a_1(a_0g(f-a_1)+a_1a_4)} \end{pmatrix}, \\ w_2 &: \begin{pmatrix} \kappa_1 & \nu_1 & \nu_3 & \nu_5 & \nu_7 \\ \frac{\kappa_2\nu_5}{\nu_6} & \nu_2 & \nu_4 & \frac{\nu_5^2}{\nu_6} & \nu_8 \end{pmatrix}; f \sim \begin{pmatrix} a_0a_2 & a_1a_2 & \frac{1}{a_2} \\ a_3 & a_4 & g \end{pmatrix}; f, \end{aligned}$$

$$\begin{aligned}
w_3 &: \left(\begin{array}{cccc} \frac{\kappa_1^3 \kappa_2^4}{(\nu_1 \nu_2 \nu_3 \nu_5 \nu_6 \nu_8)^2} & \nu_1 & \nu_3 & \nu_5 & \nu_7 \\ \frac{\kappa_1^2 \kappa_2^3}{(\nu_1 \nu_2 \nu_3 \nu_5 \nu_6 \nu_8)^2} & \nu_2 & \nu_4 & \nu_6 & \nu_8 \end{array} ; \right. \\
&\quad \left. \frac{\kappa_1 \kappa_2^2 f (g(\nu_1 \nu_5 \nu_8 (\kappa_2 (f + g \nu_2 \nu_3) - \nu_2 \nu_3 \nu_5) - \kappa_1 \kappa_2^2) + \kappa_1 \kappa_2 \nu_5) (g(\nu_1 \nu_6 \nu_8 (\kappa_2 (f + g \nu_2 \nu_3) - \nu_2 \nu_3 \nu_6) - \kappa_1 \kappa_2^2) + \kappa_1 \kappa_2 \nu_6)}{(\nu_1 \nu_8)^2 (\nu_2 \nu_3 \nu_5 \nu_6) (f g \kappa_2^2 + \nu_2 \nu_3 (g \kappa_2 - \nu_5) (g \kappa_2 - \nu_6)) (f g \nu_1 \nu_5 \nu_6 \nu_8 + \kappa_1 (g \kappa_2 - \nu_5) (g \kappa_2 - \nu_6))} \right. \\
&\quad \left. \frac{g(\kappa_1 \kappa_2)^2 (f g \kappa_2^2 + \nu_2 \nu_3 (g \kappa_2 - \nu_5) (g \kappa_2 - \nu_6))}{(\nu_2 \nu_3)^2 (\nu_1 \nu_5 \nu_6 \nu_8) (f g \nu_1 \nu_5 \nu_6 \nu_8 + \kappa_1 (g \kappa_2 - \nu_5) (g \kappa_2 - \nu_6))} \right) \\
&\sim \left(\begin{array}{ccc} a_0 & a_1 & a_2 \\ \frac{1}{a_3} & a_3^2 a_4 & \end{array} ; \begin{array}{c} \frac{a_0^2 a_1 a_2 f (a_0 g(-a_1 + f + g) - a_4 (g - a_1)) (a_0 a_2 g(-a_1 a_2 + f + g) - a_4 (g - a_1 a_2))}{(a_0 g(a_0 a_2 (f + g) - (a_2 + 1) a_4) + a_4^2) (a_0 g(a_4 (f - a_1 (a_2 + 1)) + a_0 a_1 a_2 g) + a_1 a_4^2)} \\ \frac{a_0 a_1^2 a_2 g (a_0 g(a_0 a_2 (f + g) - (a_2 + 1) a_4) + a_4^2)}{a_4 (a_0 g(a_4 (f - a_1 (a_2 + 1)) + a_0 a_1 a_2 g) + a_1 a_4^2)} \end{array} \right), \\
w_4 &: \left(\begin{array}{cccc} \frac{(\nu_4 \nu_7)^2}{\kappa_1^2} & \nu_1 & \nu_3 & \nu_5 & \nu_7 \\ \frac{\kappa_1^2 \kappa_2}{(\nu_4 \nu_7)^2} & \nu_2 & \nu_4 & \nu_6 & \nu_8 \end{array} ; \begin{array}{c} \frac{\nu_4 \nu_7 f}{\kappa_1} \\ \frac{\nu_4 \nu_7^2 (f - \nu_4) g}{\kappa_1 (\nu_7 f - \kappa_1)} \end{array} \right) \sim \left(\begin{array}{ccc} a_0 & a_1 & a_2 \\ a_3 a_4^2 & \frac{1}{a_4} & \end{array} ; \begin{array}{c} \frac{f}{a_4} \\ \frac{(f-1)g}{a_4 (f-a_4)} \end{array} \right), \\
\sigma_0 &: \left(\begin{array}{ccccc} \frac{\nu_1 \nu_2 \nu_3 \nu_4 \nu_5 \nu_6 \nu_7 \nu_8}{\kappa_1 \kappa_2^2} & \frac{\kappa_1 \kappa_2 \nu_2 \nu_3 \nu_5 \nu_7}{\nu_1 (\nu_4 \nu_6 \nu_8)^2} & \nu_3 & \nu_5 & \nu_7 \\ \frac{\kappa_2 \nu_2 \nu_3 \nu_5 \nu_7}{\nu_1 \nu_4 \nu_6 \nu_8} & \nu_2 & \nu_4 & \frac{\nu_2 \nu_3 \nu_5 \nu_6 \nu_7}{\kappa_1 \kappa_2} & \nu_8 \end{array} ; \begin{array}{c} \frac{g \nu_1 \nu_4 \nu_6 \nu_8 (\kappa_2 (f + g \nu_2 \nu_3) - \nu_2 \nu_3 \nu_6)}{\kappa_1 \kappa_2 (g \kappa_2 - \nu_6)} \\ -\frac{f \nu_1 \nu_4 \nu_6^2 \nu_8}{\kappa_1 \kappa_2 \nu_2 \nu_3 (g \kappa_2 - \nu_6)} \end{array} \right) \\
&\sim \left(\begin{array}{ccc} \frac{1}{a_2} & \frac{1}{a_1} & \frac{1}{a_0} \\ \frac{1}{a_4} & \frac{1}{a_3} & \end{array} ; \begin{array}{c} \frac{g(a_0(f+g)-a_4)}{a_1(a_0g-a_4)} \\ -\frac{a_4 f}{a_1(a_0g-a_4)} \end{array} \right), \\
\sigma_1 &: \left(\begin{array}{ccccc} \frac{(\nu_4 \nu_7)^2}{\kappa_1} & \frac{(\nu_2 \nu_3 \nu_6 \nu_7)^2}{\kappa_1 \kappa_2 \nu_4 \nu_5 \nu_8} & \nu_3 & \nu_5 & \nu_7 \\ \frac{\nu_1 \nu_5 \nu_8 (\nu_2 \nu_3 \nu_6)^2}{\kappa_1 \kappa_2^2 \nu_4} & \nu_2 & \nu_4 & \frac{\nu_1 \nu_4 \nu_5 \nu_6 \nu_8}{\kappa_1 \kappa_2} & \nu_8 \end{array} ; \begin{array}{c} \frac{\nu_4 (g \kappa_2 (f - \nu_4) + \nu_4 \nu_6)}{f \nu_6} \\ \frac{f g \kappa_2^2 \nu_4}{(\nu_2 \nu_3)^2 \nu_6 (g \kappa_2 - \nu_6)} \end{array} \right) \\
&\sim \left(\begin{array}{ccc} \frac{1}{a_0} & \frac{1}{a_2} & \frac{1}{a_1} \\ \frac{1}{a_3} & \frac{1}{a_4} & \end{array} ; \begin{array}{c} \frac{a_0 (f-1)g + a_4}{a_4 f} \\ \frac{a_0^2 f g}{a_4 (a_0 g - a_4)} \end{array} \right), \\
\sigma_2 &: \left(\begin{array}{ccccc} \frac{\kappa_1 \kappa_2^2 \nu_4 \nu_7}{\nu_1 \nu_2 \nu_3 \nu_6 \nu_8} & \frac{(\nu_2 \nu_3 \nu_6 \nu_7)^2}{\kappa_1 \kappa_2 \nu_4 \nu_5 \nu_8} & \nu_3 & \nu_5 & \nu_7 \\ \frac{(\nu_2 \nu_3)^2 \nu_5 \nu_6}{\kappa_2 \nu_4^2} & \nu_2 & \nu_4 & \frac{\kappa_1 \kappa_2 \nu_5}{\nu_1 \nu_4 \nu_6 \nu_8} & \nu_8 \end{array} ; \begin{array}{c} -\frac{\kappa_2 \nu_4 (g(f \nu_1 \nu_6 \nu_8 - \kappa_1 \kappa_2) + \kappa_1 \nu_6)}{g \nu_1 \nu_2 \nu_3 \nu_6 \nu_8 (g \kappa_2 - \nu_6)} \\ \frac{f g \kappa_2^2 \nu_4}{(\nu_2 \nu_3)^2 \nu_6 (g \kappa_2 - \nu_6)} \end{array} \right) \\
&\sim \left(\begin{array}{ccc} a_2 & a_0 & a_1 \\ a_4 & a_3 & \end{array} ; \begin{array}{c} -\frac{a_0 (f-a_1)g + a_1 a_4}{g(a_0g-a_4)} \\ \frac{a_0^2 f g}{a_4 (a_0g-a_4)} \end{array} \right).
\end{aligned}$$

The proof is standard, see [DFS20, DT18] for similar computations explained in detail. Note that reflection automorphisms σ_0 and σ_1 change the sign of the symplectic form, and so a_i changes to a_i^{-1} . We also remark that to compute the evolution of the parameters κ_i and γ_j , we use the evolution of the root variables a_i . Recall that there is redundancy in the full set of parameters κ_i and γ_j in [KNY17] for this point configuration. We first express some of them in terms of the others and the root variables a_i using (2.2) — there are various choices but they are equivalent up to changing the overall normalization. We put

$$\kappa_1 = a_4 \cdot \nu_4 \nu_7, \quad \kappa_2 = \frac{a_0 a_2}{a_4} \cdot \frac{\nu_2 \nu_3 \nu_5}{\nu_4}, \quad \nu_1 = \frac{a_0}{a_1} \cdot \frac{\nu_2 \nu_3 \nu_7}{\nu_4 \nu_8}, \quad \nu_6 = a_2 \cdot \nu_5. \quad (2.6)$$

Then, for w_0 , the root variables evolve as $\bar{a}_0 = 1/a_0$, $\bar{a}_1 = a_0 a_1$, $\bar{a}_2 = a_0 a_2$, $\bar{a}_3 = a_3$, $\bar{a}_4 = a_4$, and so, for example,

$$\bar{\kappa}_2 = \frac{\bar{a}_0 \bar{a}_2}{\bar{a}_4} \cdot \frac{\nu_2 \nu_3 \nu_5}{\nu_4} = \frac{a_2}{a_4} \cdot \frac{\nu_2 \nu_3 \nu_5}{\nu_4} = \frac{\kappa_2}{a_0} = \frac{\nu_2 \nu_3 \nu_6 \nu_7}{\kappa_1},$$

where we used (2.2) again at the last step. Other computations are similar.

2.1.3 The discrete Painlevé equation [0001̄1] on the q-P $(E_3^{(1)}/A_5^{(1)}; a)$ Surface Family

In [KNY17] the evolution for all multiplicative cases is induced by the evolution of parameters

$$\bar{\kappa}_1 = \frac{\kappa_1}{q}, \quad \bar{\kappa}_2 = q\kappa_2, \quad \text{where } q = \frac{\kappa_1^2 \kappa_2^2}{\nu_1 \nu_2 \nu_3 \nu_4 \nu_5 \nu_6 \nu_7 \nu_8}. \quad (2.7)$$

This induces the following evolution on the root variables (2.2):

$$\bar{a}_0 = a_0, \quad \bar{a}_1 = a_1, \quad \bar{a}_2 = a_2, \quad \bar{a}_3 = qa_3, \quad \bar{a}_4 = \frac{a_4}{q},$$

that in turn induces the translation (1.4) on the symmetry roots,

$$\psi_* : \alpha = \langle \alpha_0, \alpha_1, \alpha_2; \alpha_3, \alpha_4 \rangle \mapsto \psi_*(\alpha) = \alpha + \langle 0, 0, 0; -1, 1 \rangle \delta.$$

Using the standard techniques, again see [DFS20, DT18], this translation element can be expressed in terms of the generators of $\widetilde{W}(E_3^{(1)})$ as $\psi = \sigma_2^3 \circ w_3 = w_4 \circ \sigma_2^3$, resulting in the mapping

$$\psi(f, g) = \left(-\frac{\nu_2 \nu_3 \nu_4 (\kappa_2 g - \nu_5) (\kappa_2 g - \nu_6)}{\kappa_2^2 f g}, \frac{\nu_2 \nu_3 \nu_4 \nu_5 \nu_6 \nu_7 (\nu_1 \nu_5 \nu_6 \nu_8 f g + \kappa_1 (\kappa_2 g - \nu_5) (\kappa_2 g - \nu_6))}{(\kappa_1 \kappa_2)^2 g (\kappa_2^2 (f + \nu_2 \nu_3 g) g - \nu_2 \nu_3 (\kappa_2 (\nu_5 + \nu_6) g - \nu_5 \nu_6))} \right),$$

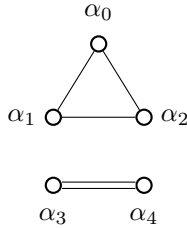
which is equivalent to [KNY17, (8.11)],

$$f\bar{f} = -\nu_2 \nu_3 \nu_4 \frac{\left(g - \frac{\nu_5}{\kappa_2}\right) \left(g - \frac{\nu_6}{\kappa_2}\right)}{g}, \quad g\bar{g} = \frac{\kappa_1}{\nu_1 \nu_2 \nu_3 \nu_8} \frac{f - \frac{\kappa_1}{\nu_7}}{f - \nu_4},$$

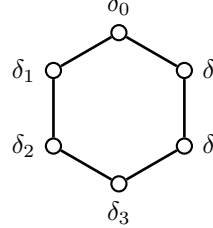
see also [Sak07, (2.13–2.14)] and the q -P_{IV} \rightarrow P_{IV} degeneration in [Sak01].

2.2 The q-P $(E_3^{(1)}/A_5^{(1)}; b)$ Surface Family

Let us now turn our attention to the (b)-model that corresponds to the choice of root bases for the surface and symmetry sub-lattices shown on Figure 6.



$$\begin{aligned} \alpha_0 &= \mathcal{H}_f + \mathcal{H}_g - \mathcal{E}_{2367}, \\ \alpha_1 &= \mathcal{H}_f - \mathcal{E}_{48}, \\ \alpha_2 &= \mathcal{H}_g - \mathcal{E}_{15}, \\ \alpha_3 &= \mathcal{H}_f + \mathcal{H}_g - \mathcal{E}_{2358} \\ \alpha_4 &= \mathcal{H}_f + \mathcal{H}_g - \mathcal{E}_{1467}, \end{aligned}$$



$$\begin{aligned} \delta_0 &= \mathcal{H}_f - \mathcal{E}_{12}, \\ \delta_1 &= \mathcal{E}_2 - \mathcal{E}_3, \\ \delta_2 &= \mathcal{H}_g - \mathcal{E}_{24}, \\ \delta_3 &= \mathcal{H}_f - \mathcal{E}_{56}, \\ \delta_4 &= \mathcal{E}_6 - \mathcal{E}_7, \\ \delta_5 &= \mathcal{H}_g - \mathcal{E}_{68}; \end{aligned} \quad (2.8)$$

Figure 6: The symmetry (left) and the surface (right) root bases for the q-P $(E_3^{(1)}/A_5^{(1)}; b)$

2.2.1 The point configuration

The decomposition of the anti-canonical divisor class into the classes of irreducible components δ_i above,

$$-\mathcal{K}_{\mathcal{X}} = [H_f - E_1 - E_2] + [E_2 - E_3] + [H_g - E_2 - E_4] + [H_f - E_5 - E_6] + [E_6 - E_7] + [H_g - E_6 - E_8],$$

can be realized by the point configuration on Figure 7 where the coordinates of the base points are again given in terms of the the [KNY17] parameters κ_i, ν_j :

$$p_1 \left(\frac{1}{f} = 0, g = \frac{1}{\nu_1} \right), p_2 \left(\frac{1}{f} = 0, \frac{1}{g} = 0 \right) \leftarrow p_3 \left(\frac{1}{f} = 0, \frac{f}{g} = -\nu_2\nu_3 \right), p_4 \left(f = \nu_4, \frac{1}{g} = 0 \right),$$

$$p_5 \left(f = 0, g = \frac{\nu_5}{\kappa_2} \right), p_6 (f = 0, g = 0) \leftarrow p_7 \left(f = 0, \frac{g}{f} = -\frac{\nu_6\nu_7}{\kappa_1\kappa_2} \right), p_8 \left(f = \frac{\kappa_1}{\nu_8}, g = 0 \right).$$

Using the same symplectic form $\omega = \frac{df \wedge dg}{fg}$ as in the (a)-case, we see that in this case the root variables are slightly different,

$$a_0 = \frac{\kappa_1\kappa_2}{\nu_2\nu_3\nu_6\nu_7}, a_1 = \frac{\kappa_1}{\nu_4\nu_8}, a_2 = \frac{\kappa_2}{\nu_1\nu_5}, a_3 = \frac{\kappa_1\kappa_2}{\nu_2\nu_3\nu_5\nu_8}, a_4 = \frac{\kappa_1\kappa_2}{\nu_1\nu_4\nu_6\nu_7}, \quad (2.9)$$

but they satisfy the same constraint $a_0a_1a_2 = a_3a_4 = q$ as before. Using the root variables, the coordinates of the base points are

$$p_1 \left(\frac{1}{f} = 0, g = \frac{1}{\nu_1} \right), p_2 \left(\frac{1}{f} = 0, \frac{1}{g} = 0 \right) \leftarrow p_3 \left(\frac{1}{f} = 0, \frac{f}{g} = -\frac{a_4}{a_0}\nu_1\nu_4 \right), p_4 \left(f = \nu_4, \frac{1}{g} = 0 \right),$$

$$p_5 \left(f = 0, g = \frac{1}{a_2\nu_1} \right), p_6 (f = 0, g = 0) \leftarrow p_7 \left(f = 0, \frac{g}{f} = -\frac{1}{a_4\nu_1\nu_4} \right), p_8 (f = a_1\nu_4, g = 0).$$

where the free parameters ν_1 and ν_4 can again be set to 1 using the rescaling action.

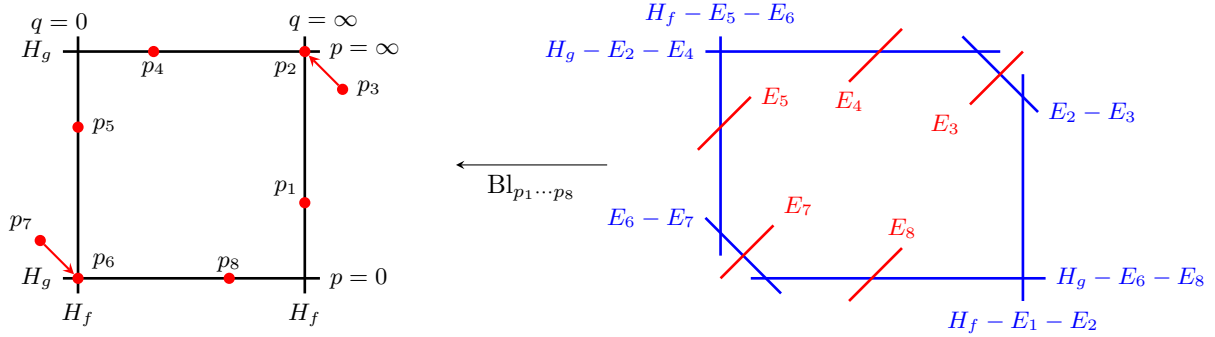


Figure 7: The model type (b) Sakai surface for the q-P $\left(E_3^{(1)}/A_5^{(1)} \right)$ family

2.2.2 The extended affine Weyl symmetry group

Since the geometric realization of our surface has changed, the birational representation will change as well. In particular, even though the action of the automorphisms σ_i on the symmetry and surface roots is the same as on Figure 5, its realization on $\text{Pic}(\mathcal{X})$ is different,

$$\sigma_0 = w_{\mathcal{E}_5 - \mathcal{E}_7} \circ w_{\mathcal{E}_4 - \mathcal{E}_8} \circ w_{\mathcal{E}_1 - \mathcal{E}_3} \circ w_{\mathcal{E}_2 - \mathcal{E}_6} \circ w_{\mathcal{H}_f - \mathcal{E}_2 - \mathcal{E}_6},$$

$$\sigma_1 = w_{\mathcal{E}_5 - \mathcal{E}_8} \circ w_{\mathcal{E}_1 - \mathcal{E}_4} \circ w_{\mathcal{H}_f - \mathcal{H}_g}.$$

The birational representation of $\widetilde{W}(E_3^{(1)}) = \text{Aut}(E_3^{(1)}) \ltimes W(E_3^{(1)})$ on the (b)-family of surfaces is described in the next Lemma.

Lemma 5. *Generators of the extended affine Weyl group $\widetilde{W}(E_3^{(1)})$ transform an initial point configuration in the (b)-model, expressed in both the KNY parameters and the root variables as*

$$\left(\begin{array}{cccccc} \kappa_1 & \nu_1 & \nu_3 & \nu_5 & \nu_7 & f \\ \kappa_2 & \nu_2 & \nu_4 & \nu_6 & \nu_8 & g \end{array} ; \right) \sim \left(\begin{array}{ccc} a_0 & a_1 & a_2 \\ a_3 & a_4 & \end{array} ; \begin{array}{c} f \\ g \end{array} \right), \quad (2.10)$$

by changing the parameters and the affine coordinates (f, g) as follows:

$$\begin{aligned} w_0 : & \left(\begin{array}{cccccc} \frac{\kappa_1^2 \kappa_2}{\nu_2 \nu_3 \nu_6 \nu_7} & \nu_1 & \nu_3 & \nu_5 & \nu_7 & \frac{\kappa_1 \kappa_2 f (f + \nu_2 \nu_3 g)}{\nu_2 \nu_3 (\nu_6 \nu_7 f + \kappa_1 \kappa_2 g)} \\ \frac{\kappa_1 \kappa_2^2}{\nu_2 \nu_3 \nu_6 \nu_7} & \nu_2 \left(\frac{\kappa_1 \kappa_2}{\nu_2 \nu_3 \nu_6 \nu_7} \right)^2 & \nu_4 & \nu_6 \left(\frac{\kappa_1 \kappa_2}{\nu_2 \nu_3 \nu_6 \nu_7} \right)^2 & \nu_8 & \frac{\nu_6 \nu_7 g (f + \nu_2 \nu_3 g)}{\nu_6 \nu_7 f + \kappa_1 \kappa_2 g} \end{array} ; \right) \\ & \sim \left(\begin{array}{ccc} \frac{1}{a_0} & a_0 a_1 & a_0 a_2 \\ a_3 & a_4 & \end{array} ; \begin{array}{c} \frac{f(a_0 f + a_4 g)}{f + a_4 g} \\ \frac{g(a_0 f + a_4 g)}{a_0 (f + a_4 g)} \end{array} \right), \\ w_1 : & \left(\begin{array}{cccccc} \frac{(\nu_4 \nu_8)^2}{\kappa_1} & \nu_1 & \nu_3 & \nu_5 & \nu_7 & \frac{\nu_4 \nu_8 f}{\kappa_1} \\ \frac{\kappa_1 \kappa_2}{\nu_4 \nu_8} & \frac{\nu_2 \nu_4 \nu_8}{\kappa_1} & \nu_4 & \frac{\nu_4 \nu_6 \nu_8}{\kappa_1} & \nu_8 & \frac{\nu_8 (f - \nu_4) g}{\nu_8 f - \kappa_1} \end{array} ; \right) \sim \left(\begin{array}{ccc} a_0 a_1 & \frac{1}{a_1} & a_1 a_2 \\ a_3 & a_4 & \end{array} ; \begin{array}{c} \frac{f}{a_1} \\ \frac{(f-1)g}{(f-a_1)} \end{array} \right), \\ w_2 : & \left(\begin{array}{cccccc} \frac{\kappa_1 \kappa_2}{\nu_1 \nu_5} & \nu_1 & \nu_3 & \nu_5 & \nu_7 & \frac{\kappa_2 f (\nu_1 g - 1)}{\nu_1 (\kappa_2 g - \nu_5)} \\ \frac{(\nu_1 \nu_5)^2}{\kappa_2} & \frac{\nu_1 \nu_2 \nu_5}{\kappa_2} & \nu_4 & \frac{\nu_1 \nu_5 \nu_6}{\kappa_2} & \nu_8 & \frac{\kappa_2 g}{\nu_1 \nu_5} \end{array} ; \right) \sim \left(\begin{array}{ccc} a_0 a_2 & a_1 a_2 & \frac{1}{a_2} \\ a_3 & a_4 & \end{array} ; \begin{array}{c} \frac{a_2 f (g-1)}{a_2 g - 1} \\ a_2 g \end{array} \right), \\ w_3 : & \left(\begin{array}{cccccc} \kappa_1 & \nu_1 & \nu_3 & \nu_5 & \nu_7 & \frac{\kappa_1 \kappa_2 f (\nu_8 (f + \nu_2 \nu_3 g) - \kappa_1)}{\nu_2 \nu_3 \nu_8 (\nu_5 \nu_8 f + \kappa_1 (\kappa_2 g - \nu_5))} \\ \kappa_2 & \nu_2 \left(\frac{\kappa_1 \kappa_2}{\nu_2 \nu_3 \nu_5 \nu_8} \right)^2 & \nu_4 & \nu_6 \left(\frac{\nu_2 \nu_3 \nu_5 \nu_8}{\kappa_1 \kappa_2} \right)^2 & \nu_8 & \frac{\nu_5 \nu_8 g (\kappa_2 f + \nu_2 \nu_3 (\kappa_2 g - \nu_5))}{\kappa_2 (\nu_5 \nu_8 f + \kappa_1 (\kappa_2 g - \nu_5))} \end{array} ; \right) \\ & \sim \left(\begin{array}{ccc} a_0 & a_1 & a_2 \\ \frac{1}{a_3} & a_3^2 a_4 & \end{array} ; \begin{array}{c} \frac{a_1 a_2 f (a_0 (f - a_1) + a_4 g)}{a_4 (f + a_1 (a_2 g - 1))} \\ \frac{g (a_0 a_2 f + a_4 (a_2 g - 1))}{a_0 a_2 (f + a_1 (a_2 g - 1))} \end{array} \right), \\ w_4 : & \left(\begin{array}{cccccc} \kappa_1 & \nu_1 & \nu_3 & \nu_5 & \nu_7 & \frac{\nu_4 \nu_6 \nu_7 f (f - \nu_1 g (f - \nu_4))}{\nu_4 \nu_6 \nu_7 f - \kappa_1 \kappa_2 g (f - \nu_4)} \\ \kappa_2 & \nu_2 \left(\frac{\nu_1 \nu_4 \nu_6 \nu_7}{\kappa_1 \kappa_2} \right)^2 & \nu_4 & \nu_6 \left(\frac{\kappa_1 \kappa_2}{\nu_1 \nu_4 \nu_6 \nu_7} \right)^2 & \nu_8 & \frac{\kappa_1 \kappa_2 g (f - \nu_1 g (f - \nu_4))}{\nu_1 \nu_4 (f (1 - \nu_1 g) + \kappa_1 \kappa_2 g)} \end{array} ; \right) \\ & \sim \left(\begin{array}{ccc} a_0 & a_1 & a_2 \\ a_3 a_4^2 & \frac{1}{a_4} & \end{array} ; \begin{array}{c} \frac{f (f + g - f g)}{f - a_4 (f - 1) g} \\ \frac{a_4 g (f g - f - g)}{f (g - 1) - a_4 g} \end{array} \right), \\ \sigma_0 : & \left(\begin{array}{cccccc} \frac{(\nu_4 \nu_8)^2}{\kappa_1} & \nu_1 & \nu_3 & \nu_5 & \nu_7 & \frac{\nu_4 \nu_8 f}{\kappa_1} \\ \frac{\nu_1 \nu_2 \nu_3 \nu_5 \nu_6 \nu_7}{\kappa_1 \kappa_2} & \frac{\nu_2 \nu_4 \nu_8}{\kappa_1} & \nu_4 & \frac{\nu_4 \nu_6 \nu_8}{\kappa_1} & \nu_8 & -\frac{f}{\nu_1 \nu_2 \nu_3 g} \end{array} ; \right) \sim \left(\begin{array}{ccc} \frac{1}{a_2} & \frac{1}{a_1} & \frac{1}{a_0} \\ \frac{1}{a_4} & \frac{1}{a_3} & \end{array} ; \begin{array}{c} \frac{f}{a_1} \\ -\frac{a_0 f}{a_4 g} \end{array} \right), \\ \sigma_1 : & \left(\begin{array}{cccccc} \frac{\nu_1 \nu_4 \nu_5 \nu_8}{\kappa_2} & \nu_1 & \nu_3 & \nu_5 & \nu_7 & \nu_1 \nu_4 g \\ \frac{\nu_1 \nu_4 \nu_5 \nu_8}{\kappa_1} & \frac{(\nu_1 \nu_4)^2}{\nu_2 \nu_3^2} & \nu_4 & \frac{(\nu_5 \nu_8)^2}{\nu_6 \nu_7^2} & \nu_8 & \frac{f}{\nu_1 \nu_4} \end{array} ; \right) \sim \left(\begin{array}{ccc} \frac{1}{a_0} & \frac{1}{a_2} & \frac{1}{a_1} \\ \frac{1}{a_3} & \frac{1}{a_4} & \end{array} ; \begin{array}{c} g \\ f \end{array} \right), \\ \sigma_2 : & \left(\begin{array}{cccccc} \frac{\kappa_1 \kappa_2 \nu_4 \nu_8}{\nu_2 \nu_3 \nu_6 \nu_7} & \nu_1 & \nu_3 & \nu_5 & \nu_7 & -\frac{\nu_4 f}{\nu_2 \nu_3 g} \\ \frac{\kappa_1 \nu_1 \nu_5}{\nu_4 \nu_8} & \frac{\kappa_1 \nu_1^2 \nu_4}{\nu_2 \nu_3^2 \nu_8} & \nu_4 & \frac{\kappa_1 \nu_5^2 \nu_8}{\nu_4 \nu_6 \nu_7^2} & \nu_8 & \frac{\nu_8 f}{\kappa_1 \nu_1} \end{array} ; \right) \sim \left(\begin{array}{ccc} a_2 & a_0 & a_1 \\ a_4 & a_3 & \end{array} ; \begin{array}{c} -\frac{a_0 f}{a_4 g} \\ \frac{f}{a_1} \end{array} \right). \end{aligned}$$

The proof of this Lemma is similar to Lemma 4. Note that we use the following root variable parameterization, obtained from (2.9):

$$\kappa_1 = a_1 \nu_4 \nu_8, \quad \kappa_2 = a_2 \nu_1 \nu_5, \quad \nu_2 = \frac{a_4}{a_0} \frac{\nu_1 \nu_4}{\nu_3}, \quad \nu_6 = \frac{a_1 a_2}{a_4} \frac{\nu_5 \nu_8}{\nu_7}.$$

2.2.3 The discrete Painlevé equation [01 $\bar{1}$ 00] on the q -P $(E_3^{(1)}/A_5^{(1)}; b)$ Surface Family

The evolution of parameters (2.7) induces the following evolution on the root variables (2.9):

$$\bar{a}_0 = a_0, \quad \bar{a}_1 = \frac{a_1}{q}, \quad \bar{a}_2 = qa_2, \quad \bar{a}_3 = a_3, \quad \bar{a}_4 = a_4,$$

that in turn induces the translation (1.5) on the symmetry roots,

$$\phi_* : \alpha = \langle \alpha_0, \alpha_1, \alpha_2; \alpha_3, \alpha_4 \rangle \mapsto \phi_*(\alpha) = \alpha + \langle 0, 1, -1; 0, 0 \rangle \delta.$$

This translation can be expressed in terms of the generators as $\phi = \sigma_2^4 \circ w_0 \circ w_2 = w_1 \circ w_0 \circ \sigma_2^4$, resulting in the mapping

$$\phi(f, g) = \left(-\frac{\nu_1 \nu_2 \nu_3 \nu_4 g (\kappa_2 g - \nu_5)}{\kappa_2 f (\nu_1 g - 1)}, \frac{\nu_1 \nu_2 \nu_3 \nu_4 (\kappa_2 g - \nu_5) (\nu_5 \nu_6 \nu_7 f (\nu_1 g - 1) + \kappa_1 \kappa_2 g (\kappa_2 g - \nu_5))}{\kappa_1 \kappa_2^2 f (\nu_1 g - 1) (\kappa_2 f (\nu_1 g - 1) + \nu_1 \nu_2 \nu_3 g (\kappa_2 g - \nu_5))} \right),$$

which is equivalent to [KNY17, (8.14)],

$$f\bar{f} = -\nu_2 \nu_3 \nu_4 \frac{g \left(g - \frac{\nu_5}{\kappa_2} \right)}{g - \frac{1}{\nu_1}}, \quad g\bar{g} = -\frac{1}{\nu_1 \nu_2 \nu_3} \frac{f \left(f - \frac{\kappa_1}{\nu_8} \right)}{f - \nu_4},$$

see also [Sak07, (2.15–2.16)] and the q -P_{III} \rightarrow P_{III} degeneration in [Sak01].

3 The Identification Procedure

In this section we follow the procedure introduced in [DFS20] to formally identify recurrence (1.3) as a discrete Painlevé equation. This procedure consists of several steps that can be grouped into two parts. The first part is geometric, where we first resolve the singularities of the mapping, linearize the mapping on the Picard lattice of the resulting algebraic surface, determine the decomposition of the unique anti-canonical divisor into irreducible components whose intersection configuration is described by an affine Dynkin diagram. The type of this diagram is known as the surface type of the equation in the Sakai classification scheme. We do this part in Section 3.1.

The second part is algebraic, where we do some preliminary change of basis between the Picard lattices of our surface and of one of the model examples so that the surface roots match. This allows us to obtain the expressions for the standard symmetry roots in terms of the basis of the Picard lattice of our q -Laguerre surface. Using the evolution on the Picard lattice we can determine the translation direction and see if it is conjugate to one of the known examples. If so, we can do that conjugation to find the final correspondence between the bases of these two Picard lattices and then determine the underlying change of coordinates. We do this part in Section 3.2, except that in our case the q -Laguerre dynamic is conjugated to a composition of two standard mappings.

Since the procedure we follow here is by now quite standard, we only outline the computations and refer the interested reader to [DFS20] and [KNY01] for details.

3.1 Resolving the Singularities, Identifying the Surface Type, and Linearizing the Dynamics on the Picard Lattice

We begin by regularizing the mapping given by recurrence (1.3). Note that this recurrence defines two half-step mappings, the forward half-step $\varphi_1^{(n)} : (x_n, y_n) \mapsto (x_n, y_{n+1})$, where

$$y_{n+1} = \frac{q^{2n+1} Q(T - x_n)(x_n - 1) + x_n(x_n y_n - 1)}{x_n^2(x_n y_n - 1)}, \quad (3.1)$$

and the backward half-step $\varphi_2^{(n)} : (x_n, y_n) \mapsto (x_{n-1}, y_n)$, where

$$x_{n-1} = \frac{(y - q^n)(x_n y_n - 1) - q^{2n} Q (T y_n - 1)(y_n - 1)}{y_n (y_n - q^n)(x_n y_n - 1)}. \quad (3.2)$$

Each mapping is clearly birational, and so after inverting one of them we obtain the full forward and backward mappings $\varphi^{(n)} = (\varphi_2^{(n+1)})^{-1} \circ \varphi_1^{(n)} : (x_n, y_n) \mapsto (x_{n+1}, y_{n+1})$ and $(\varphi^{(n)})^{-1} = (\varphi_1^{(n-1)})^{-1} \circ \varphi_2^{(n)}$. The explicit expressions for these mappings are complicated and we omit them.

Extending these mappings to the compactification $\mathbb{P}^1 \times \mathbb{P}^1$ and using the standard techniques described, e.g., in [DFS20] or [HDC20], we get the following base points of the mappings shown on Figure 8 (left)

$$\begin{aligned} q_1(x=1, y=1), \quad q_2\left(x=T, y=\frac{1}{T}\right), \\ q_3\left(x=0, \frac{1}{y}=0\right) \leftarrow q_4\left(x=0, \frac{1}{xy}=0\right) \leftarrow q_5\left(x=0, \frac{1}{x^2 y}=\frac{q^{-2n-1}}{QT}\right), \\ q_6\left(\frac{1}{x}=0, y=0\right) \leftarrow q_7\left(\frac{1}{x}=0, xy=1-q^n Q\right), \quad q_8\left(\frac{1}{x}=0, y=q^n\right). \end{aligned} \quad (3.3)$$

Note that the points q_1, q_2, q_3 , and q_6 lie on the (1,1) curve given by the equation $xy - 1 = 0$ in the affine (x, y) -chart. Next, modifying the geometry by applying the blowup procedure at the base points, we extend each mapping from a birational transformation of $\mathbb{C} \times \mathbb{C}$ to an isomorphism on the family of Sakai surfaces parameterized by q, Q, T , and n and described schematically on Figure 8 (right).

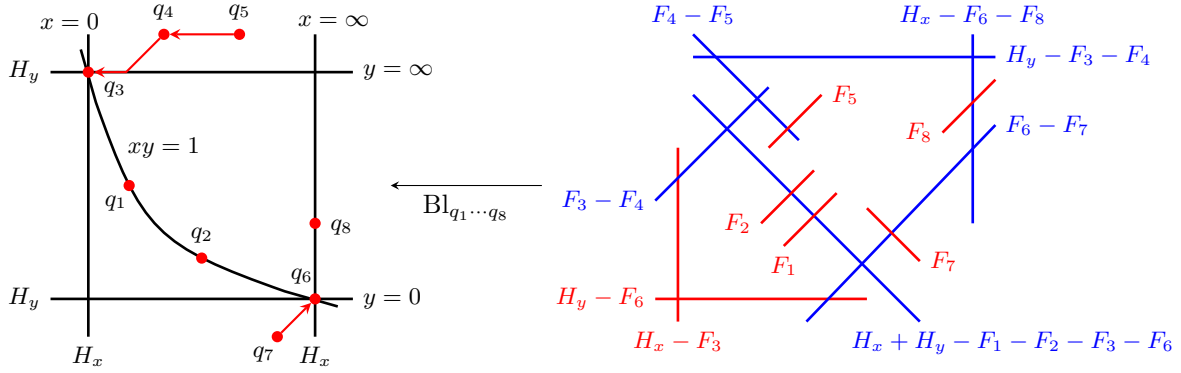
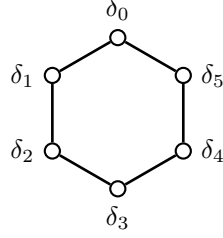


Figure 8: The Sakai surface for the q -Laguerre recurrence

Recall that the key object in the geometric approach to Painlevé equations is the *Picard lattice* of this surface family. It is well-known that the Picard lattice of $\mathbb{P}^1 \times \mathbb{P}^1$ is generated by the classes of the coordinate lines, $\text{Pic}(\mathbb{P}^1 \times \mathbb{P}^1) = \text{Span}_{\mathbb{Z}}\{\mathcal{H}_x, \mathcal{H}_y\}$. Each blowup is a surgery that adds a class of the exceptional divisor $\mathcal{F}_i = [F_i]$ to the Picard lattice and so for each surface \mathcal{X} in the family we get $\text{Pic}(\mathcal{X}) = \text{Span}_{\mathbb{Z}}\{\mathcal{H}_x, \mathcal{H}_y, \mathcal{F}_1, \dots, \mathcal{F}_8\}$. This lattice is equipped with the *intersection product* defined on the generators by $\mathcal{H}_x \bullet \mathcal{H}_x = \mathcal{H}_y \bullet \mathcal{H}_y = \mathcal{H}_x \bullet \mathcal{F}_i = \mathcal{H}_y \bullet \mathcal{F}_j = 0$, $\mathcal{H}_x \bullet \mathcal{H}_y = 1$, and $\mathcal{F}_i \bullet \mathcal{F}_j = -\delta_{ij}$. Using this inner product we can assign to each curve on \mathcal{X} its *self-intersection* index, e.g., all exceptional curves F_i have index -1 ; such curves are marked in red on Figure 8 (right). But there are other curves with self-intersection index -1 , in particular, proper transforms $\mathcal{H}_i - F_j$ of the coordinate lines passing through the blowup points. There are infinitely many -1 curves, but curves with higher negative self-intersection index are more special. Usually, as is in our case, there are only finitely many curves with self-intersection index -2 that are the *irreducible components of the unique anti-canonical divisor class of canonical type* (the generalized Halphen surface condition, see [Sak01]). Such curves are marked in blue on Figure 8 (right) and their intersection

configuration is described by an affine Dynkin diagram which in our case is $A_5^{(1)}$, see Figure 9. This is the *surface type* of our recurrence.



$$\begin{aligned}
\delta_0 &= \mathcal{F}_3 - \mathcal{F}_4, & \delta_3 &= \mathcal{H}_x - \mathcal{F}_6 - \mathcal{F}_8, \\
\delta_1 &= \mathcal{F}_4 - \mathcal{F}_5, & \delta_4 &= \mathcal{F}_6 - \mathcal{F}_7, \\
\delta_2 &= \mathcal{H}_y - \mathcal{F}_3 - \mathcal{F}_4, & \delta_5 &= \mathcal{H}_x + \mathcal{H}_y - \mathcal{F}_1 - \mathcal{F}_2 - \mathcal{F}_3 - \mathcal{F}_6.
\end{aligned} \tag{3.4}$$

Figure 9: The initial surface root basis for the q -Laguerre recurrence

We can also see the action of the dynamic on the standard basis of the Picard lattice. This is a direct computation summarized in the following Lemma.

Lemma 6. *The induced linear action of the full mapping φ_* on the Picard lattice is given by*

$$\begin{aligned}
\mathcal{H}_x &\mapsto \overline{\mathcal{H}}_x + 3\overline{\mathcal{H}}_y - \overline{\mathcal{F}}_{123678}, & \mathcal{H}_y &\mapsto 3\overline{\mathcal{H}}_x + 6\overline{\mathcal{H}}_y - 2\overline{\mathcal{F}}_{1237} - \overline{\mathcal{F}}_{45} - 3\overline{\mathcal{F}}_{68}, \\
\mathcal{F}_1 &\mapsto \overline{\mathcal{H}}_x + 2\overline{\mathcal{H}}_y - \overline{\mathcal{F}}_{23678}, & \mathcal{F}_2 &\mapsto \overline{\mathcal{H}}_x + 2\overline{\mathcal{H}}_y - \overline{\mathcal{F}}_{13678}, \\
\mathcal{F}_3 &\mapsto \overline{\mathcal{H}}_x + 3\overline{\mathcal{H}}_y - \overline{\mathcal{F}}_{1235678}, & \mathcal{F}_4 &\mapsto \overline{\mathcal{H}}_x + 3\overline{\mathcal{H}}_y - \overline{\mathcal{F}}_{1234678}, \\
\mathcal{F}_5 &\mapsto \overline{\mathcal{H}}_x + 2\overline{\mathcal{H}}_y - \overline{\mathcal{F}}_{12678}, & \mathcal{F}_6 &\mapsto \overline{\mathcal{H}}_x + 2\overline{\mathcal{H}}_y - \overline{\mathcal{F}}_{12368}, \\
\mathcal{F}_7 &\mapsto \overline{\mathcal{H}}_y - \overline{\mathcal{F}}_8, & \mathcal{F}_8 &\mapsto \overline{\mathcal{H}}_y - \overline{\mathcal{F}}_6,
\end{aligned}$$

where we use the notation $\mathcal{F}_{i\dots j} = \mathcal{F}_i + \dots + \mathcal{F}_j$. The evolution of parameters (hence, the base points) is as expected, $\mathbf{b} = \{T, Q, q, n\} \mapsto \overline{\mathbf{b}} = \{T, Q, q, n + 1\}$.

The next step is to see if we can match this equation to one of the standard examples. We do it in the next section.

3.2 Matching the Geometry to a Standard Model and Identifying the Equation

As we have seen in Section 2, there are two standard geometric realizations of this surface given in [KNY17], termed *(a)-model* and *(b)-model*. Both realizations are birationally equivalent, but given that the birational representation using the (b)-model, given in Lemma 5, is somewhat simpler than the one for the (a)-model given in Lemma 4, we match our geometry to the one of (b)-model described in Section 2.2.1. This is done in three steps. First, we make some initial change of basis between the Picard lattices for our surface and that of a standard example. This can be done by matching the surface roots on Figure 3.4 with the one for the (b)-model shown on the right on Figure 2.8. There are of course many different ways to do so, but at this point it is enough to find *some* identification that we can later adjust using diagram automorphism elements from $\widetilde{W}(E_3^{(1)})$. For example, we can just match the nodes with the same indices on these two diagrams,

$$\begin{aligned}
\delta_0 &= \mathcal{F}_3 - \mathcal{F}_4 = \mathcal{H}_f - \mathcal{E}_1 - \mathcal{E}_2, & \delta_3 &= \mathcal{H}_x - \mathcal{F}_6 - \mathcal{F}_8 = \mathcal{H}_f - \mathcal{E}_5 - \mathcal{E}_6, \\
\delta_1 &= \mathcal{F}_4 - \mathcal{F}_5 = \mathcal{E}_2 - \mathcal{E}_3, & \delta_4 &= \mathcal{F}_6 - \mathcal{F}_7 = \mathcal{E}_6 - \mathcal{E}_7, \\
\delta_2 &= \mathcal{H}_y - \mathcal{F}_3 - \mathcal{F}_4 = \mathcal{H}_g - \mathcal{E}_2 - \mathcal{E}_4, & \delta_5 &= \mathcal{H}_x + \mathcal{H}_y - \mathcal{F}_1 - \mathcal{F}_2 - \mathcal{F}_3 - \mathcal{F}_6 = \mathcal{H}_g - \mathcal{E}_6 - \mathcal{E}_8,
\end{aligned}$$

which can be done via the change of basis

$$\begin{aligned}
\mathcal{H}_f &= \mathcal{H}_x, & \mathcal{E}_1 &= \mathcal{H}_x - \mathcal{F}_3, & \mathcal{E}_3 &= \mathcal{F}_5, & \mathcal{E}_5 &= \mathcal{F}_8, & \mathcal{E}_7 &= \mathcal{F}_7, \\
\mathcal{H}_g &= \mathcal{H}_x + \mathcal{H}_y - \mathcal{F}_2 - \mathcal{F}_3, & \mathcal{E}_2 &= \mathcal{F}_4, & \mathcal{E}_4 &= \mathcal{H}_x - \mathcal{F}_2, & \mathcal{E}_6 &= \mathcal{F}_6, & \mathcal{E}_8 &= \mathcal{F}_1.
\end{aligned} \tag{3.5}$$

Using this identification we get the symmetry roots for the q -Laguerre recurrence corresponding to the (b)-model symmetry roots shown on the left on Figure 2.8,

$$\begin{aligned}
\alpha_0 &= \mathcal{H}_f + \mathcal{H}_g - \mathcal{E}_2 - \mathcal{E}_3 - \mathcal{E}_6 - \mathcal{E}_7 &= 2\mathcal{H}_x + \mathcal{H}_y - \mathcal{F}_2 - \mathcal{F}_3 - \mathcal{F}_4 - \mathcal{F}_5 - \mathcal{F}_6 - \mathcal{F}_7 \\
\alpha_1 &= \mathcal{H}_f - \mathcal{E}_4 - \mathcal{E}_8 &= \mathcal{F}_2 - \mathcal{F}_1, \\
\alpha_2 &= \mathcal{H}_g - \mathcal{E}_1 - \mathcal{E}_5 &= \mathcal{H}_y - \mathcal{F}_2 - \mathcal{F}_8, \\
\alpha_3 &= \mathcal{H}_f + \mathcal{H}_g - \mathcal{E}_2 - \mathcal{E}_3 - \mathcal{E}_5 - \mathcal{E}_8 &= 2\mathcal{H}_x + \mathcal{H}_y - \mathcal{F}_1 - \mathcal{F}_2 - \mathcal{F}_3 - \mathcal{F}_4 - \mathcal{F}_5 - \mathcal{F}_8, \\
\alpha_4 &= \mathcal{H}_f + \mathcal{H}_g - \mathcal{E}_1 - \mathcal{E}_4 - \mathcal{E}_6 - \mathcal{E}_7 &= \mathcal{H}_y - \mathcal{F}_6 - \mathcal{F}_7.
\end{aligned} \tag{3.6}$$

Now we can, using the action of φ_* on $\text{Pic}(\mathcal{X})$ given in Lemma 6, identify the translation element on the symmetry sublattice;

$$\varphi_* : \alpha = \langle \alpha_0, \alpha_1, \alpha_2; \alpha_3, \alpha_4 \rangle \mapsto \varphi_*(\alpha) = \alpha + \langle -1, 0, 1; -1, 1 \rangle \delta.$$

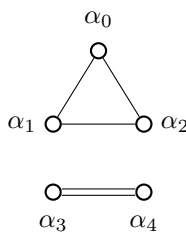
From this we immediately see that the q -Laguerre dynamic is *not conjugated* to either of the standard examples, since it occurs on both sublattices, but it is almost the same as their composition, we just need to adjust the change of basis, which is the second step.

Consider the automorphism σ_2^2 , see Figure 5, which acts on the symmetry roots as

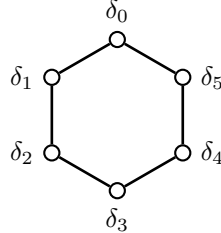
$$\sigma_2^2(\langle \alpha_0, \alpha_1, \alpha_2; \alpha_3, \alpha_4 \rangle) = \langle \alpha_2, \alpha_0, \alpha_1; \alpha_3, \alpha_4 \rangle,$$

so it transforms the dynamic into $[01\bar{1}\bar{1}1]$, and that is the composition of two standard translations. Acting by this automorphism on our change of basis creates a somewhat less obvious change of basis,

$$\begin{aligned}
\mathcal{H}_f &= \mathcal{H}_x + \mathcal{H}_y - \mathcal{F}_2 - \mathcal{F}_3, & \mathcal{H}_x &= \mathcal{H}_f + \mathcal{H}_g - \mathcal{E}_2 - \mathcal{E}_6, \\
\mathcal{H}_g &= 2\mathcal{H}_x + \mathcal{H}_y - \mathcal{F}_2 - \mathcal{F}_3 - \mathcal{F}_4 - \mathcal{F}_6, & \mathcal{H}_y &= 2\mathcal{H}_f + \mathcal{H}_g - \mathcal{E}_2 - \mathcal{E}_4 - \mathcal{E}_6 - \mathcal{E}_7, \\
\mathcal{E}_1 &= \mathcal{F}_7, & \mathcal{F}_1 &= \mathcal{E}_3, \\
\mathcal{E}_2 &= \mathcal{H}_x + \mathcal{H}_y - \mathcal{F}_2 - \mathcal{F}_3 - \mathcal{F}_6, & \mathcal{F}_2 &= \mathcal{H}_f + \mathcal{H}_g - \mathcal{E}_2 - \mathcal{E}_6 - \mathcal{E}_7, \\
\mathcal{E}_3 &= \mathcal{F}_1, & \mathcal{F}_3 &= \mathcal{H}_f + \mathcal{H}_g - \mathcal{E}_2 - \mathcal{E}_4 - \mathcal{E}_6, \\
\mathcal{E}_4 &= \mathcal{H}_x - \mathcal{F}_3, & \mathcal{F}_4 &= \mathcal{H}_f - \mathcal{E}_6, \\
\mathcal{E}_5 &= \mathcal{F}_5, & \mathcal{F}_5 &= \mathcal{E}_5, \\
\mathcal{E}_6 &= \mathcal{H}_x + \mathcal{H}_y - \mathcal{F}_2 - \mathcal{F}_3 - \mathcal{F}_4, & \mathcal{F}_6 &= \mathcal{H}_f - \mathcal{E}_2, \\
\mathcal{E}_7 &= \mathcal{H}_x - \mathcal{F}_2, & \mathcal{F}_7 &= \mathcal{E}_1, \\
\mathcal{E}_8 &= \mathcal{F}_8, & \mathcal{F}_8 &= \mathcal{E}_8.
\end{aligned} \tag{3.7}$$



$$\begin{aligned}
\alpha_0 &= \mathcal{F}_2 - \mathcal{F}_1, \\
\alpha_1 &= \mathcal{H}_y - \mathcal{F}_{28}, \\
\alpha_2 &= 2\mathcal{H}_x + \mathcal{H}_y - \mathcal{F}_{234567}, \\
\alpha_3 &= 2\mathcal{H}_x + \mathcal{H}_y - \mathcal{F}_{123456}, \\
\alpha_4 &= \mathcal{H}_y - \mathcal{F}_{67},
\end{aligned}$$



$$\begin{aligned}
\delta_0 &= \mathcal{F}_6 - \mathcal{F}_7, \\
\delta_1 &= \mathcal{H}_x + \mathcal{H}_y - \mathcal{F}_{1236} \\
\delta_2 &= \mathcal{F}_3 - \mathcal{F}_4, \\
\delta_3 &= \mathcal{F}_4 - \mathcal{F}_5, \\
\delta_4 &= \mathcal{H}_y - \mathcal{F}_{34}, \\
\delta_5 &= \mathcal{H}_x - \mathcal{F}_{68}.
\end{aligned} \tag{3.8}$$

Figure 10: The final choice of the symmetry (left) and the surface (right) root bases for the q -Laguerre surface

Applying the change of basis (3.7) to the root bases for the (b)-model surface on Figure 6 we get the adjusted root bases for the q -Laguerre recurrence shown on Figure 10.

Now the action of the mapping φ on the symmetry roots α_i becomes

$$\varphi_* : \alpha = \langle \alpha_0, \alpha_1, \alpha_2; \alpha_3, \alpha_4 \rangle \mapsto \varphi_*(\alpha) = \alpha + \langle 0, 1, -1; -1, 1 \rangle \delta = (\phi_* \circ \psi_*)(\alpha) = (\psi_* \circ \phi_*)(\alpha). \quad (3.9)$$

We can express φ in terms of generators of the extended affine Weyl group $\widetilde{W}(E_3^{(1)})$ as

$$\varphi = \sigma_1 \circ \sigma_0 \circ w_3 \circ w_0 \circ w_2 = \psi \circ \phi = (w_4 \circ \sigma_2^3) \circ (\sigma_2^4 \circ w_0 \circ w_2) \quad (3.10)$$

Remark 7. Given that $\varphi = \varphi_2^{-1} \circ \varphi_1$, see (3.1)–(3.2), it is a natural question whether this decomposition is the same as $\varphi = \psi \circ \phi$. A quick reflection suggest that this can not be the case, and indeed, we can compute that

$$\begin{aligned} (\varphi_1)_*(\alpha) &= \langle -\alpha_0, \alpha_0 + \alpha_2, \alpha_0 + \alpha_1; \alpha_4, \alpha_3 \rangle, & \varphi_1 &= \sigma_0 \circ \sigma_2^2 \circ w_0 \\ (\varphi_2)_*(\alpha) &= \langle -\alpha_0, -\alpha_1, 2\alpha_0 + 2\alpha_1 + \alpha_2; \alpha_3 + 2\alpha_4, -\alpha_4 \rangle, & \varphi_2 &= \sigma_0 \circ \sigma_2 \circ w_4 \circ w_0 \circ w_1 \circ w_0, \end{aligned}$$

and so the backward map φ_2 acts on both components of the $E_3^{(1)}$ affine Dynkin diagram.

The final step is to determine the explicit change of coordinates. For that, we also need to compute the root variables for the q -Laguerre case, which is done in the following Lemma.

Lemma 8. The points q_1, \dots, q_8 lie on the polar divisor of the symplectic form ω that, in the affine (x, y) -chart, is given by

$$\omega = k \frac{dx \wedge dy}{xy - 1} \quad (3.11)$$

(i) The residues of the symplectic form ω along the irreducible components d_i of the polar divisor corresponding to the surface roots $\delta_i = [d_i]$, given in (3.8), are

$$\begin{aligned} \text{res}_{d_0} \omega &= -k \frac{dv_6}{v_6 - 1}, & \text{res}_{d_2} \omega &= k \frac{dv_3}{v_3(v_3 - 1)}, & \text{res}_{d_4} \omega &= k \frac{dx}{x}, \\ \text{res}_{d_1} \omega &= k \frac{dy}{y}, & \text{res}_{d_3} \omega &= -k \frac{dv_4}{v_4}, & \text{res}_{d_5} \omega &= -k \frac{dy}{y}, \end{aligned}$$

(ii) For the standard root variable normalization $\exp(\chi(\delta)) = a_0 a_1 a_2 = a_3 a_4 = q$ we need to take $k = -1$ and the root variables a_i are then given by

$$a_0 = T, \quad a_1 = \frac{1}{q^n T}, \quad a_2 = q^{n+1}; \quad a_3 = q^{n+1} Q, \quad a_4 = \frac{1}{q^n Q}. \quad (3.12)$$

Note that the discrete time evolution $n \mapsto n + 1$ induces the evolution

$$\bar{a}_0 = a_0, \quad \bar{a}_1 = \frac{a_1}{q}, \quad \bar{a}_2 = qa_2; \quad \bar{a}_3 = qa_3, \quad \bar{a}_4 = \frac{a_4}{q}$$

matching the translation (3.9) (recall that the evolution of the root variables is dual to the evolution of the roots).

Proof is a direct computation and is omitted. We are now in the position to determine the birational change of variables identifying the q -Laguerre surfaces with the standard Sakai surface using the (b)-model. It is given in the following Lemma.

Lemma 9. The Sakai surface shown on Figure 8 can be matched with the (b)-model shown on Figure 7 via the following explicit change of coordinates and parameter identification:

$$\left\{ \begin{array}{l} x_n(f, g) = -\frac{f_n}{g_n \nu_2 \nu_3}, \\ y_n(f, g) = -\frac{\nu_2 \nu_3}{\kappa_1 \kappa_2} \frac{\kappa_1 \kappa_2 g_n (f_n - \nu_4) - \nu_4 \nu_6 \nu_7}{f_n^2}, \\ T = \frac{\kappa_1 \kappa_2}{\nu_2 \nu_3 \nu_6 \nu_7}, \quad Q = \frac{\kappa_1 \nu_1}{\nu_2 \nu_3 \nu_8}, \\ q^n = \frac{\nu_2 \nu_3 \nu_4 \nu_6 \nu_7 \nu_8}{\kappa_1^2 \kappa_2}, \end{array} \right. \quad \left\{ \begin{array}{l} f_n(x, y) = \nu_4 \frac{x_n - T}{T(x_n y_n - 1)}, \\ g_n(x, y) = -\frac{\nu_4}{\nu_2 \nu_3} \frac{x_n - T}{T x_n (x_n y_n - 1)}, \\ \kappa_1 = \frac{\nu_4 \nu_8}{q^n T}, \quad \kappa_2 = \frac{\nu_2 \nu_3 \nu_5 q^{2n+1} Q T}{\nu_4}, \\ \nu_1 = \frac{q^n Q T \nu_2 \nu_3 \nu_5}{\nu_4}, \quad \nu_6 = \frac{q^{n+1} Q \nu_5 \nu_8}{T \nu_7}, \end{array} \right. \quad (3.13)$$

As before, we can rescale the parameters $\nu_2\nu_3$ and ν_4 to be equal to 1, the remaining parameters ν_i do not play a role in the variable change and get canceled in the birational representation.

Proof. The parameter matching is done via the root variables expressions (2.9) and (3.12). We get the explicit change of coordinates from the change of basis (3.7) in the Picard lattice. Let us briefly recall the key steps using the simplest case. To find $x(f, g)$ we need to find the basis of the pencil of $(1, 1)$ -curves $|H_x| = |H_f + H_g - \mathcal{E}_2 - \mathcal{E}_6|$ on the (f, g) -plane passing through the points $p_2(\infty, \infty)$ and $p_6(0, 0)$ on Figure 7, which has the form $a_{10}f + a_{01}g = 0$. A homogeneous coordinate on this pencil is $[f : g]$, which coincides with x up to some Möbius transformation. Thus,

$$x(f, g) = \frac{Af + Bg}{Cf + Dg}.$$

We determine the coefficients A, \dots, D using the mapping of the exceptional divisors. For example,

$$[(f = 0)] = \mathcal{H}_f - \mathcal{E}_5 - \mathcal{E}_6 = \mathcal{F}_4 - \mathcal{F}_5,$$

so in affine charts the map should collapse $f = 0$ to $q_3(0, \infty) \leftarrow q_4$. Thus, $B = 0$. Similarly, $g = 0$ should map to $x = \infty$, and so $C = 0$. Thus, $x(f, g) = (Af)/(Dg) = A(f/g)$, since we can, without loss of generality, put $D = 1$. To find A we note that p_3 should map to q_1 , and thus $x(f, g)(p_3) = A(f/g)(p_3) = Av_3(p_3) = A(-\nu_2\nu_3) = 1$, so $A = -(\nu_2\nu_3)^{-1}$. Other computations are done along the same lines, but are more involved, see [DFS20] or [HDC20] for more detailed examples. \square

Remark 10. Using the birational representation of $\widetilde{W}(E_3^{(1)})$, we can write the mapping $\varphi = \sigma_1 \circ \sigma_0 \circ w_3 \circ w_0 \circ w_2$ explicitly. For simplicity, we write it using the root variables of the (b) -model, but it is still quite complicated,

$$\varphi(f, g) = \left(\frac{f(a_0a_2(f(1-g) + a_1(a_2g - 1)) + a_4g(1 - a_2g))}{a_0a_1a_2g(a_2g - 1)(a_0a_2f - a_4(1 - a_2g))}, \right. \\ \left. \frac{f(a_0a_2f(g-1) + a_4g(a_2g - 1))(a_0a_2(f(g-1) - a_1(a_2g - 1)) + a_4g(a_2g - 1))}{a_4(a_2g - 1)(a_0a_2f(f(g-1) + a_1(a_2g - 1)(a_0a_2g - 1)) + a_4g(a_2g - 1)(f + a_0a_1a_2(a_2g - 1)))} \right) \quad (3.14)$$

It is straightforward to verify that the change of coordinates (3.13) transforms this mapping into our recurrence (1.3), when expressed in the evolutionary form. The dynamic in parameters κ_i and ν_j can be obtained using (2.9).

4 Conclusions

In this paper we studied a recurrence relation appearing in the study of deformed q -Laguerre orthogonal polynomials and identified it as a discrete Painlevé equation on the $A_5^{(1)}$ family of Sakai surfaces. An interesting feature of this example is that this equation in a composition of two standard mappings, and so recognizing it as such without the use of geometric techniques may be very difficult, if not impossible. In contrast, the geometric identification procedure makes this process quite straightforward and effectively removes any guesswork. Given that this deformed q -Laguerre dynamic is a composition of a discrete q -P_{IV} and discrete q -P_{III} equations, it is an interesting follow-up question to see if it has a good continuous limit.

References

- [Ask89] Richard Askey, *Orthogonal polynomials and theta functions*, Theta functions—Bowdoin 1987, Part 2 (Brunswick, ME, 1987), Proc. Sympos. Pure Math., vol. 49, Part 2, Amer. Math. Soc., Providence, RI, 1989, pp. 299–321. MR 1013179

- [BVA10] Lies Boelen and Walter Van Assche, *Discrete Painlevé equations for recurrence coefficients of semiclassical Laguerre polynomials*, Proc. Amer. Math. Soc. **138** (2010), no. 4, 1317–1331. MR 2578525
- [BVA15] ———, *Variations of Stieltjes-Wigert and q -Laguerre polynomials and their recurrence coefficients*, J. Approx. Theory **193** (2015), 56–73. MR 3324563
- [CG15] Yang Chen and James Griffin, *Non linear difference equations arising from a deformation of the q -Laguerre weight*, Indag. Math. (N.S.) **26** (2015), no. 1, 266–279. MR 3281704
- [CI10] Yang Chen and Alexander Its, *Painlevé III and a singular linear statistics in Hermitian random matrix ensembles. I*, J. Approx. Theory **162** (2010), no. 2, 270–297. MR 2581382
- [CL98] Yang Chen and Nigel Lawrence, *Density of zeros of some orthogonal polynomials*, Methods Appl. Anal. **5** (1998), no. 4, 367–386. MR 1669863
- [DFS20] Anton Dzhamay, Galina Filipuk, and Alexander Stokes, *Recurrence coefficients for discrete orthogonal polynomials with hypergeometric weight and discrete Painlevé equations*, J. Phys. A **53** (2020), no. 49, 495201, 29. MR 4188771
- [DFS22] ———, *Differential equations for the recurrence coefficients of semiclassical orthogonal polynomials and their relation to the Painlevé equations via the geometric approach*, Stud. Appl. Math. **148** (2022), no. 4, 1656–1702. MR 4433344
- [DT18] Anton Dzhamay and Tomoyuki Takenawa, *On some applications of Sakai’s geometric theory of discrete Painlevé equations*, SIGMA Symmetry Integrability Geom. Methods Appl. **14** (2018), Paper No. 075, 20. MR 3830210
- [HDC20] Jie Hu, Anton Dzhamay, and Yang Chen, *Gap probabilities in the Laguerre unitary ensemble and discrete Painlevé equations*, J. Phys. A **53** (2020), no. 35, 354003, 18. MR 4137540
- [KNY01] Kenji Kajiwara, Masatoshi Noumi, and Yasuhiko Yamada, *A study on the fourth q -Painlevé equation*, J. Phys. A **34** (2001), no. 41, 8563–8581. MR 1876614
- [KNY17] ———, *Geometric aspects of Painlevé equations*, J. Phys. A **50** (2017), no. 7, 073001, 164. MR 3609039
- [LDFZ22] Xing Li, Anton Dzhamay, Galina Filipuk, and Da-jun Zhang, *Recurrence relations for the generalized Laguerre and Charlier orthogonal polynomials and discrete painlevé equations on the $D_6^{(1)}$ Sakai surface*, 2022.
- [Mag95] Alphonse P. Magnus, *Painlevé-type differential equations for the recurrence coefficients of semiclassical orthogonal polynomials*, Proceedings of the Fourth International Symposium on Orthogonal Polynomials and their Applications (Evian-Les-Bains, 1992), vol. 57, 1995, pp. 215–237. MR 1340938
- [Meh04] Madan Lal Mehta, *Random matrices*, third ed., Pure and Applied Mathematics (Amsterdam), vol. 142, Elsevier/Academic Press, Amsterdam, 2004. MR MR2129906 (2006b:82001)
- [Moa81] Daniel S. Moak, *The q -analogue of the Laguerre polynomials*, J. Math. Anal. Appl. **81** (1981), no. 1, 20–47. MR 618759
- [Sak01] Hidetaka Sakai, *Rational surfaces associated with affine root systems and geometry of the Painlevé equations*, Comm. Math. Phys. **220** (2001), no. 1, 165–229. MR 1882403

- [Sak07] ———, *Problem: discrete Painlevé equations and their Lax forms*, Algebraic, analytic and geometric aspects of complex differential equations and their deformations. Painlevé hierarchies, RIMS Kôkyûroku Bessatsu, B2, Res. Inst. Math. Sci. (RIMS), Kyoto, 2007, pp. 195–208. MR 2310030 (2008c:33020)
- [VA18] Walter Van Assche, *Orthogonal polynomials and Painlevé equations*, Australian Mathematical Society Lecture Series, vol. 27, Cambridge University Press, Cambridge, 2018. MR 3729446
- [VA22] ———, *Orthogonal polynomials, Toda lattices and Painlevé equations*, Phys. D **434** (2022), Paper No. 133214, 9. MR 4396612